Study and Implementation of a Sandwich Structure as a Stiffener to a Trailing Edge Panel

Tiago José Gomes da Costa
tiago.da.costa@tecnico.ulisboa.pt

Instituto Superior Técnico, Lisboa, Portugal

November 2014

Abstract

This work was made in collaboration with the company OGMA that manufactures the trailing edge panel in composite material of an aircraft's wing. This study aims to validate the possibility of changing the stiffeners shape of this structure. The panel is composed by nine stiffeners whose configuration requires an excessive amount of work during the manufacture process, which can be eased by changing the stiffeners to a Sandwich structure with a foam core. To support this new shape, both stiffeners were studied with the Classical Laminated Plate Theory and the Finite Element Method. Finally, a study of the cross sections was performed to guarantee that the required flat areas size is maintained and 22 specimens were manufactured in order to test and validate the results.
Keywords: Composite Materials, stiffener, Sandwich, Classical Laminated Plate Theory, Finite Element Method.

1. Introduction

The current shape of the stiffeners is composed by a flat skin with seven layers of composite material and six layers forming an upside-down T, known by T-Stiffener (Figure 1). This configuration is manufactured with two autoclave cycles, the first for curing the skin and the second for simultaneously cure and bond the layers of the stiffener with an adhesive. In this last operation, tools are needed to keep the layers of the stiffener in the right place.

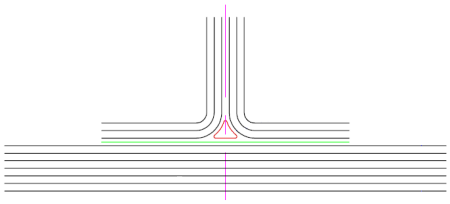

Figure 1: Cross section of the T-Stiffener.

A Sandwich structure, as represented in Figure 2, needs only one autoclave cycle in which all the composite layers are cured with the foam core (known as BEAD) and the adhesive inside. Two different cores are available, being the difference between them the radius of the foam (0.625 and 0.750 inches). In order to save composite material, there is interest in proving that the BEAD with the smallest radius has the same or higher resistance than the current configuration.

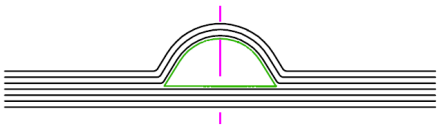

Figure 2: Cross section of the stiffener with the foam core.

By decreasing the number of cure cycles from two to one, the manufacture process becomes easier and the probability of future defects due to the cure process is decreased. However, it has to be proven that the new stiffener is capable of supporting the same kind of loads and, if possible, has higher resistance to failure under bending.

2. Composite Materials

A composite material is the result of mixing two or more different materials with a well defined boundary between them [1]. In aerospace industry, it is common to use combinations of carbon or graphite fibers as a reinforcing phase and a matrix of a thermosetting resin of the epoxy group. This combination allows the achievement of a high ratio between structural resistance and weight that, in many components, would not be possible if metallic materials were used. Nowadays, composite materials are used in many aircraft components, such as trailing edge panels, control surfaces, floor panels, fairings and main landing gear doors [2].

The basic unity of a laminated composite material is a lamina formed by a combination of fibers placed in a homogeneous matrix. While the fibers are responsible for supporting the loads, the matrix keeps them together, protects them from environmental conditions and acts like a medium of transferring loads between the fibers.

A lamina is named according to the way fibers are placed, and they can be unidirectional, bidirectional and woven fabric. This last arrangement has fibers running simultaneously in transversal (*fill*) and longitudinal (*warp*) directions and tangled in a certain pattern. Woven fabric laminae lay better in structural configurations with substantial curvature and are more durable during handling [3].

Using a single lamina for a structure would lead to an ineffective project due to its small thickness and the fact that some laminae have reduced stiffness and resistance in transverse direction. Therefore, a laminate is built by stacking several laminae in the direction of the thickness with different orientations.

2.1. Sandwich Structure

A Sandwich structure consists of two facesheets of composite material separated by a lightweight core [4]. Usually, the core and the facesheets are bonded with an adhesive. There is a variety of materials and configurations used for the core depending on the application and the desired properties: foam (as is the case of this study), honeycomb and even low density aluminum. The foam may be treated as an isotropic body, which is not the case of an honeycomb core whose properties depend on the direction.

In general, the purpose of the core is to increase the bending stiffness by moving material away from the neutral axis of the section. The stiffness and strength of the core are usually much lower than those of the facesheets. However, it must be strong enough not to collapse under pressure during cure.

Although this type of structure allows the increase of bending properties without significant weight penalty, it may bring additional failure modes related to the presence of the core and the adhesive.

2.2. Classical Laminated Plate Theory

A lamina of composite material is anisotropic with its properties depending on the direction. It may also be considered orthotropic with three mutual planes of elastic symmetry [5]. If the thickness is negligible compared to other dimensions, a state of plane stress may be assumed and the Hooke′s Law for this kind of materials is given by

$$\begin{bmatrix}\sigma_1\\ \sigma_2\\ \tau_{12}\end{bmatrix} = \begin{bmatrix}Q_{11} & Q_{12} & 0\\ Q_{12} & Q_{22} & 0\\ 0 & 0 & Q_{66}\end{bmatrix}\begin{bmatrix}\varepsilon_1\\ \varepsilon_2\\ \gamma_{12}\end{bmatrix} \tag{1}$$

where 1 and 2 are the longitudinal and transverse directions, respectively. The constants Q_{ij} can be related to the engineering elastic constants of the material obtained by experimental tests:

$$Q_{11} = \frac{E_1}{1-\nu_{21}\nu_{12}} \tag{2a}$$

$$Q_{22} = \frac{E_2}{1-\nu_{21}\nu_{12}} \tag{2b}$$

$$Q_{12} = \frac{\nu_{12}E_2}{1-\nu_{21}\nu_{12}} = \frac{\nu_{21}E_1}{1-\nu_{21}\nu_{12}} \tag{2c}$$

$$Q_{66} = G_{12} \tag{2d}$$

In an unidirectional lamina, direction 1 is aligned with the longitudinal direction of the fibers while direction 2 is perpendicular to them. If the lamina has a woven configuration, 1 corresponds to the warp direction and 2 to the fill direction [6].

If the lamina is placed in such a way that the local axes do not correspond to the global axes of the laminate, a transformation of stresses and strains must be performed:

$$\begin{bmatrix}\sigma_x\\ \sigma_y\\ \tau_{xy}\end{bmatrix} = \begin{bmatrix}\bar{Q}_{11} & \bar{Q}_{12} & \bar{Q}_{16}\\ \bar{Q}_{12} & \bar{Q}_{22} & \bar{Q}_{26}\\ \bar{Q}_{16} & \bar{Q}_{26} & \bar{Q}_{66}\end{bmatrix}\begin{bmatrix}\varepsilon_x\\ \varepsilon_y\\ \gamma_{xy}\end{bmatrix} \tag{3}$$

$$\bar{Q}_{11} = Q_{11}c^4 + Q_{22}s^4 + 2\left(Q_{12}+2Q_{66}\right)s^2c^2 \tag{4a}$$

$$\bar{Q}_{12} = \left(Q_{11}+Q_{22}-4Q_{66}\right)s^2c^2 + \\ + Q_{12}\left(c^4+s^4\right) \tag{4b}$$

$$\bar{Q}_{22} = Q_{11}s^4 + Q_{22}c^4 + 2\left(Q_{12}+2Q_{66}\right)s^2c^2 \tag{4c}$$

$$\bar{Q}_{16} = \left(Q_{11}-Q_{12}-2Q_{66}\right)c^3s - \\ - \left(Q_{22}-Q_{12}-2Q_{66}\right)s^2c^2 \tag{4d}$$

$$\bar{Q}_{26} = \left(Q_{11}-Q_{12}-2Q_{66}\right)cs^3 - \\ - \left(Q_{22}-Q_{12}-2Q_{66}\right)c^3s \tag{4e}$$

$$\bar{Q}_{66} = \left(Q_{11}+Q_{22}-2Q_{12}-2Q_{66}\right)s^2c^2 + \\ + Q_{66}\left(s^4+c^4\right) \tag{4f}$$

In the previous equations, c and s are cosine and sine of the angle θ at which the lamina is placed, respectively, while x and y represent the longitudinal and transverse directions of the laminate.

The Classical Laminated Plate Theory is used to develop the relations between strain and stress [7] in a laminate by assuming that:

- Each lamina is orthotropic;
- Each lamina is homogeneous;
- A line straight and perpendicular to the middle surface remains straight and perpendicular to the middle surface during deformation;
- The laminate is thin and is loaded only in its plane (plane stress);
- Displacements are continuous and small throughout the laminate;
- Each lamina is elastic.
- No slip occurs between the lamina interfaces.

The relation between the applied loads and moments in a laminate and the respective deformation is given by the stiffness matrices, $[A]$, $[B]$ and $[D]$. This matrices represent the stiffness to elongation, coupling and bending, respectively [7].

$$\begin{bmatrix} N_x \\ N_y \\ N_{xy} \\ M_x \\ M_y \\ M_{xy} \end{bmatrix} = \begin{bmatrix} & [A] & & [B] & \\ & & & & \\ & [B] & & [D] & \end{bmatrix} \begin{bmatrix} \varepsilon_x^0 \\ \varepsilon_y^0 \\ \gamma_{xy}^0 \\ \kappa_x \\ \kappa_y \\ \kappa_{xy} \end{bmatrix} \tag{5}$$

The first column vector of Equation (5) represents the in-plane forces and moments applied to the laminate. The last vector of the previous equation contains the deformation of the mid-surface (identified by the superscript ^{0}) and the curvatures of the laminate sections.

Matrices $[A]$, $[B]$ and $[D]$ are calculated from $\bar{Q}_{ij}$ constants.

$$A_{ij} = \sum_{k=1}^{n} (Q_{ij})_k (z_k - z_{k-1}) \tag{6a}$$

$$B_{ij} = \frac{1}{2} \sum_{k=1}^{n} (Q_{ij})_k \left(z_k^2 - z_{k-1}^2\right) \tag{6b}$$

$$D_{ij} = \frac{1}{3} \sum_{k=1}^{n} (Q_{ij})_k \left(z_k^3 - z_{k-1}^3\right) \tag{6c}$$

where z_k and z_{k-1} are the top and bottom coordinates of each lamina relative to the laminate mid-plane. If the laminate is symmetric and balanced, the elastic modulus can be calculated using [A] and [D] matrixes and the total thickness of the laminate, h.

$$E_x = \frac{1}{A^{-1}(1,1) \times h} \tag{7a}$$

$$E_y = \frac{1}{A^{-1}(2,2) \times h} \tag{7b}$$

$$Ef_x = \frac{12}{D^{-1}(1,1) \times h^3} \tag{7c}$$

$$Ef_y = \frac{12}{D^{-1}(2,2) \times h^3} \tag{7d}$$

2.3. Simplified Analysis Techniques

There is a simpler way of finding the Young Modulus of a laminate based on empirical results and known as *Simplified Analysis Techniques* [1].

In a laminate composed by a woven fabric plies of carbon/graphite, laminae placed at an angle of $0°/90°$ contribute with 100% of their resistance, while a ply whose orientation is $\pm 45°$, contributes with 30% of its total resistance. Thus, the elastic modulus E of a laminate can be calculated by

$$E = \frac{E_F}{N_F} \left(N_{090} + 0.3 N_{\pm 45}\right) \tag{8}$$

where E_F is the Young Modulus of the ply, N_F is number of total plies, N_{090} and $N_{\pm 45}$ are the number of plies with orientations of $0°/90°$ and $\pm 45°$, respectively.

These formulas are usually conservative when compared to Laminated Plate Theory.

2.4. Cross-Sectional Properties

The axial (EA) and bending (EI) stiffnesses of a cross-section are very often used in design and analysis and, therefore, accurate determination of their values for composite structures is very important [4]. There are some significant differences from metal cross-sections due to the fact that, for a cross-section made using composite materials, the different members may have different layups and thus stiffnesses.

Assuming for simplicity that the lay-up of each member is symmetric and balanced, the equivalent axial and bending stiffenesses of the cross section can be calculated by summing the individual stiffenesses of each member:

$$(EA)_{eq} = \sum_i (EA)_i \tag{9}$$

$$(EI)_{eq} = \sum_i (EI)_i \tag{10}$$

where i is the *ith* member of the cross-section.

The moment of area I is calculated using the cross-section neutral axis position that may have different locations in axial or bending situations. For a uniaxial loading case with the load applied at the neutral axis, the strains in all members of the cross-section are equal. For a bending case, if a moment is applied to the section, the neutral axis is defined as the point that guarantees that the radii of curvature R_c (or the curvature κ_x) is constant for all section members [4].

$$\bar{y} = \frac{\sum(EAy)_i}{\sum(EA)_i} \tag{11}$$

E is either the membrane or bending modulus of each member.

2.5. Failure Criteria

It is difficult to predict the failure of a composite material, especially because most of the times the damage may start before the final failure. Being able to predict when damage starts and how it evolves requires individual modeling of the matrix and fibers [3].

However, there are a few methods that can be used to estimate the loads that lead to the break of a lamina in a laminate. These criteria may be based on ultimate stress or ultimate strain. Other methods, as is the Tsail-Hill criteria, take into account the interaction between different failure modes [3].

The Maximum Strain Failure Criteria was used to calculate the maximum load that the specimen can support before failure takes place. This was done comparing the ultimate strains (tensile or compressive) in lamina local reference axes to the strains obtained when a load is applied. The failure of the lamina occurs if one or more of the next conditions is met:

$$\varepsilon_1 > \varepsilon_{1u}^t \text{ (or } \varepsilon_{1u}^c) \tag{12a}$$

$$\varepsilon_2 > \varepsilon_{2u}^t \text{ (or } \varepsilon_{2u}^c) \tag{12b}$$

$$|\gamma_{12}| > \gamma_{12u} \tag{12c}$$

3. Calculation of The Stiffeners Properties

In this section, the methods for calculating and the results for the axial and bending stiffnesses of each stiffener cross-section are presented. The maximum load that can be applied to the stiffeners was also estimated by performing a Finite Element Analysis to the entire stiffener.

The composite material used to make the trailing edge panel and its stiffeners has a woven fabric configuration known as 8 Harness Satin Weave construction. This means that each yarn goes over 7 and under 1 yarn in both directions (warp and fill) [6]. A lamina like this, with its weaves perpendicular to each other, is still orthotropic and the Classical Laminated Plate Theory is valid for studying a laminate composed by these plies [5]. However, and beacause each lamina has simultaneously fibers running in two perpendicular directions, the angle of rotation of a ply must be redefined. Therefore, using the same notation as [6], θ is the angle between the fibers of the warp side and the global axis x of the laminate. This means that for a ply placed in such a way that their fibers have an orientation of $0°/90°$, θ will be equal to zero, while for a lamina with fibers running in $\pm 45°$ directions, θ is $45°$.

The properties of the composite material required for the calculations are listed in Table 1.

Property	Value
E_1 (GPa)	60.674
E_2 (GPa)	60.674
G_{12} (GPa)	5.516
ν_{12}	0.060
ν_{21}	0.060
t (mm)	0.381

Table 1: Properties of Graphite STM 22-815 TYP 3 CL2 [8].

3.1. T-Stiffener Section

Three methods were used to calculate the axial stiffness of the T-Stiffener section: Classical Laminated Plate Theory (CLPT), The Finite Element Method (FEM) and Simplified Analysis Technique (SAT). This last approach was not used for the bending stiffness calculation due to the fact that it doesn't provide means to estimate bending modulus.

3.1.1 Axial Stiffness - EA

In order to estimate the axial stiffness of the T-Stiffener cross-section, an approximation had to be done to make the calculation easier. The approximation consist in neglecting the two small radius curvature of the plies, resulting in a section like the one in Figure 3.

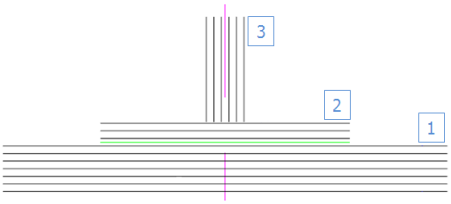

Figure 3: Approximate cross-section of T-Stiffener.

The calculation of the axial stiffness was made by estimating the elastic modulus of each member (using both CLPT and SAT methods) of the previous figure, and using them in Equation (9).

The Finite Element Method (FEM) followed a different approach. A constant cross section was modeled with ANSYS® with the finite element *SHELL181*, which has four nodes with six degrees of freedom in each one and is governed by the first-order shear-deformation theory (Mindlin-Reissner shell theory) [9]. The element allows the specification of the number of composite layers and the

orientation of each one. It is also possible to define were the reference surface should be placed, at the bottom, middle or top of the layers.

At one end of the constant section, all the degrees of freedom of nodes were constrained while at the other end two forces were applied in the x direction (Figure 4).

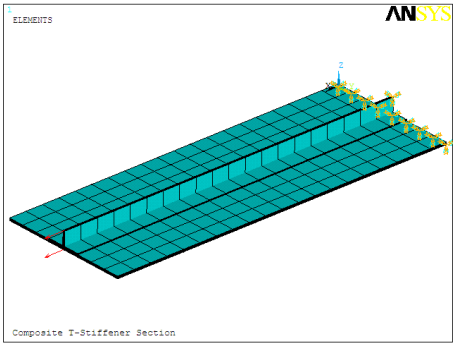

Figure 4: Finite element model of the T-Stiffener section.

The position of the neutral axis was determined by varying the intensity of the two applied forces. The pair of force intensities for each the variation of the extension of the nodes at the middle of the beam is minimal represents the position of the neutral axis. Knowing this position, it is possible to relate the average extension of the nodes to the resultant applied force in order to calculate the axial stiffness.

$$EA = \frac{P}{\varepsilon_x} \tag{13}$$

The axial stiffness (EA) calculated by three methods and the respective comparison is presented in Table 2.

Method	$EA\ (GPa.mm^2)$	**Deviation**[1] **(%)**
CLPT	22625.685	-
SAT	20243.314	10.5
FEM	22501.120	0.6

Table 2: Comparison of the EA values obtained by the three methods for the (*T-Stiffener*) section.

[1]Calculated using CLPT results as a reference.

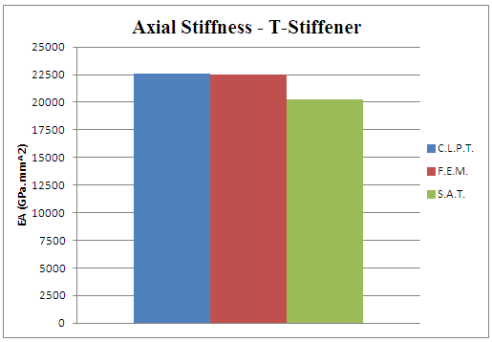

Figure 5: Comparison of the EA values obtained by the three methods for the (*T-Stiffener*) section.

It can be seen that the results from CLPT and FEM are very similar while SAT is more conservative.

3.1.2 Bending Stiffness - EI

CLPT and FEM methods were used to calculate the bending stiffness of the T-Stiffener cross-section. While CLPT allows to determine the bending modulus of each member of the section and use them in Equation (10), FEM was used in a similar way as described in subsection 3.1.1. However, instead of looking for the position of the neutral axis that guarantees a minimum variation of the extension, this time the minimum curvature variation of the section due to a constant moment was the criteria for finding both the neutral axis and bending stiffness.

The constant bending moment was simulated by applying two forces with different directions.

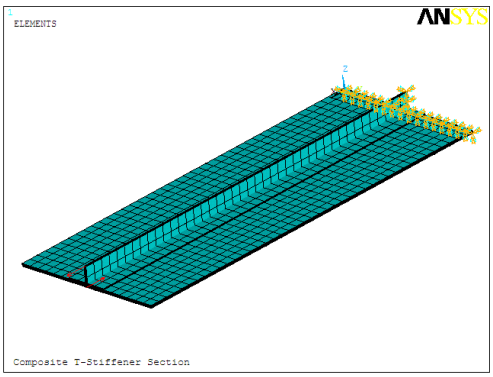

Figure 6: Finite element model of the T-Stiffener section (EI).

Knowing the value of the moment applied to the section and the average curvatures at the neutral axis, the bending stiffness was estimated by Equation (14).

$$EI = \frac{M}{\kappa_x} \tag{14}$$

The results obtained by both methods and a comparison between them is presented in Table (3) and Figure (7).

Method	**EI** $(GPa.mm^4)$	**Deviation**[2] **(%)**
CLPT	328733.894	-
FEM	314810.677	4.2

Table 3: Comparison of the EI values obtained by the three methods for the (*T-Stiffener*) section.

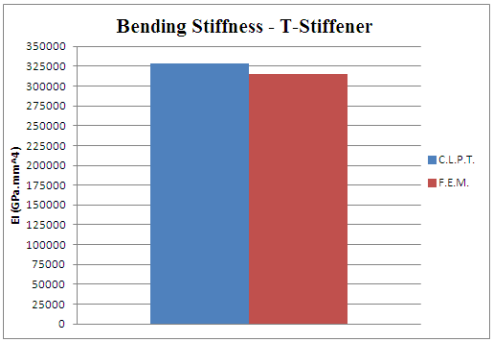

Figure 7: Comparison of the EI values obtained by two methods for the (*T-Stiffener*) section.

As it can be seen by the previous figure and table, the FEM result is about 4% lower than the one calculated from CLPT. It is a consequence of having modeled the constant section with a SHELL finite element, which doesn't take into account the thickness of the members of the section, especially the one that is at the bottom of it.

3.2. BEAD Section Properties

Due to its complex geometry and the fact that some members of the section of the stiffener with the foam core BEAD do not have a symmetrical lay-up, the properties of this stiffener were estimated using only the FEM method. The foam core was neglected, considering that the composite layers are the main structural component of the section. This also makes the analysis easier by reducing the number of finite elements.

Two different configurations were studied, one with a radius of 0.625 inches and the other with a radius of 0.750 inches. The finite element model for calculating the axial and bending stiffness, with the respective loads, are presented in the next two figures.

[2]Calculated using CLPT results as a reference.

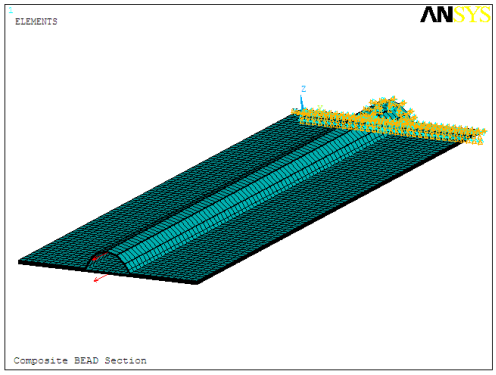

Figure 8: Finite element model of the BEAD section (EA).

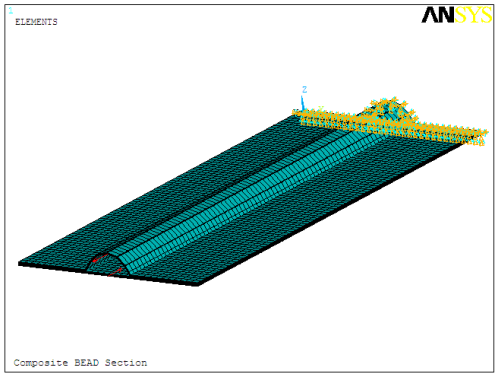

Figure 9: Finite element model of the BEAD section (EI).

The results of the Finite Element Method for these sections, after the independence with element mesh is verified, and the respective comparison with the T-Stiffener section is presented in Table 4 and Figures 10 and 11.

Section	**EA** $(GPa.mm^2)$	**EI** $(GPa.mm^4)$
T-Stiffener	22501.12	314810.677
BEAD 0.625	19165.827	390960.272
BEAD 0.750	19374.926	639588.612

Table 4: Comparison of the three sections.

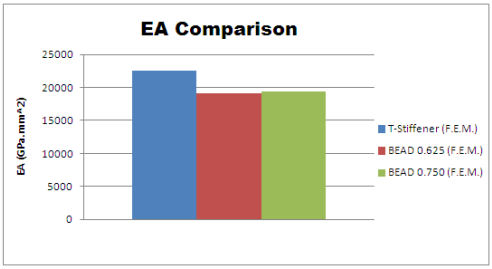

Figure 10: Axial stiffness comparison.

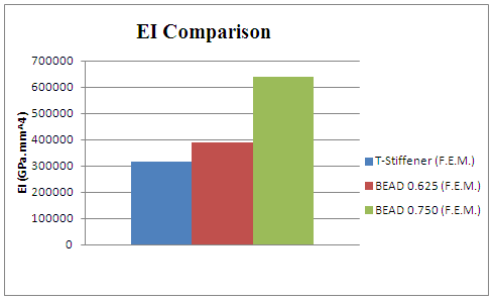

Figure 11: Bending stiffness comparison.

Two conclusions can be made from the previous Table and Figures:

- The axial stiffness (EA) of the T-Stiffener section is higher than both BEAD sections;
- The BEAD section with the smallest radius (0.625 in) has a higher bending stiffness (EI) than the T-Stiffener section.

The fact that the Sandwich configuration has a lower axial stiffness represents no problem because the panel supports allow axial movement. Therefore, the critical situation will be bending and not traction or compression.

3.3. Computational Analysis of the Specimens

The experimental tests that will validate the substitution of the stiffener configuration consist in a three point bending test with the specimen simply supported. In order to predict the maximum load that can be applied and to determine the areas where the maximum strain is expected, a finite element model of the entire stiffeners was made. Once again, the foam core was neglected due to its low mechanical properties compared to the composite layers.

The finite element used was SHELL181. ANSYS® has the ability to calculate the ratio between the resulting stress and strain in each element and the ultimate stress or strain (depending on the failure criteria used). The ultimate strains of the composite material can be found at [8] and are presented in Table 5.

Ultimate Strain	Value
ε_{1u}^{t}	0.0064
ε_{1u}^{c}	0.0059
ε_{2u}^{t}	0.0064
ε_{2u}^{c}	0.0059
ε_{12u}	0.0117

Table 5: Ultimate strains of the composite material [8].

The next three figures represent the ratio between the resulting strains and the ultimate strains of the material for each stiffener. If this ratio is equal to one somewhere in the model, it means that the at least one layer has failed due to the applied load.

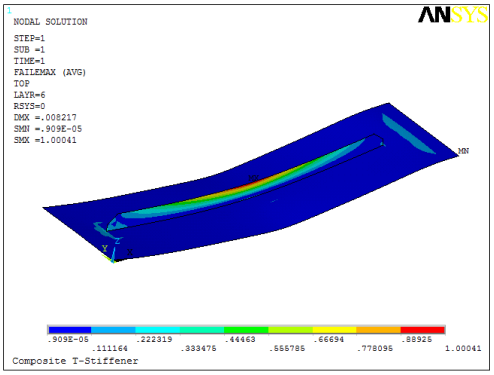

Figure 12: Maximum strain failure criteria for T-Stiffener.

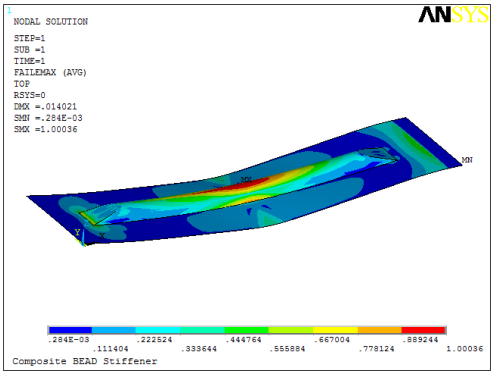

Figure 13: Maximum strain failure criteria for the stiffener BEAD 0.625.

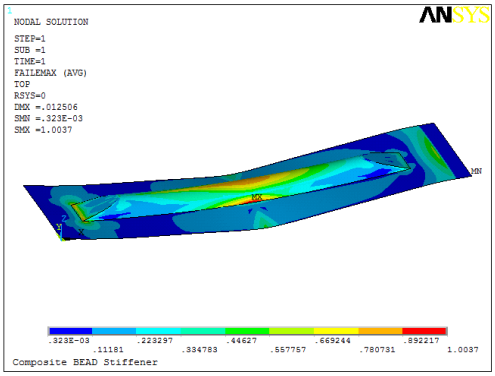

Figure 14: Maximum strain failure criteria for the stiffener BEAD 0.750.

As it can be seen by Figures 12, 13 and 14, the failure occurs at the top of the stiffener for all con-

figurations. The maximum load determined by this method for each one is presented in the Figure (15).

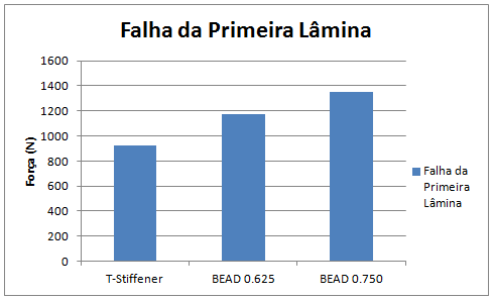

Figure 15: Comparison of the maximum load for the three specimens.

Although the foam core was not used in the calculations, the stiffeners with BEAD apparently have a higher resistance than the current configuration. However, this model is unable to predict other failure modes, such as the separation of the T-Stiffener and the skin or the crippling of the panel.

4. Specimens Manufacture

Although it was determined by theoretical methods that the Sandwich configuration with a foam core has higher resistance than the current T-Stiffener, experimental tests must be done to prove this conclusions. In this section, the manufacture of the specimens will be explained.

4.1. Dimensional Control

Despite a Sandwich construction has already been used in other components of the wing, the number of composite layers that have been chosen for the trailing edge panel is completely new. Therefore, a dimensional control study was made to check the curvature of the composite plies at the edges of the foam to guarantee that the required flat areas are kept.

Two specimens with foams of different radius were manufactured in order to check the curvatures and the thicknesses of the composite plies. These specimens were cut into several sections and each one was checked and evaluated at the microscope with the computer program *Perfect Image*®.

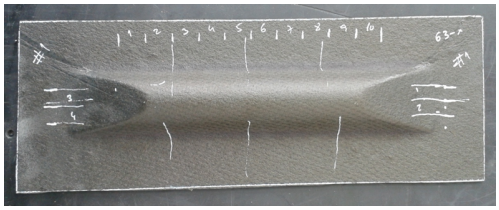

Figure 16: Specimen for dimensional control.

Both transversal and longitudinal sections were measured, as it can be seen by the following figures.

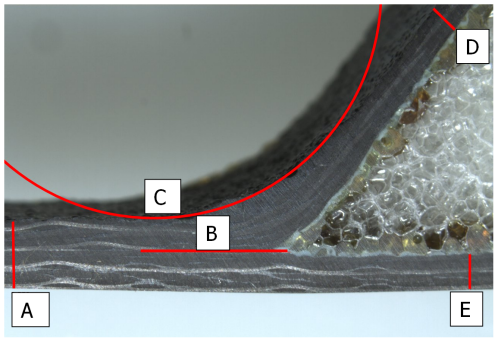

Figure 17: BEAD transversal section.

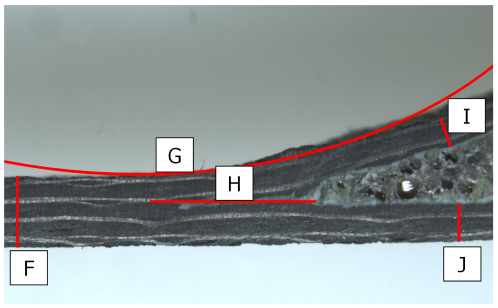

Figure 18: BEAD longitudinal section (ramp-down).

Figure 18 shows that the composite layers at the end of the BEAD only get completely horizontal after a certain distance (identified by H). This distance is about 6 millimeters at the ends of the foam for both specimens, which makes impossible to keep the required flat areas needed to guarantee the proper distance between the stiffener and the supports of the panel or adjacent stiffeners.
It was decided to manufacture the BEADs with less 6 millimeters length than the original project. This decision was also approved by the client.

4.2. Specimens Manufacture

The manufacture of the specimens followed the same steps required for building the panel, except that in the end the stiffeners were cut into individual specimens. As mentioned before, the T-Stiffener configuration is produced with two lay-ups and two autoclave cycles, the first to cure the skin and the second to simultaneously cure and bond the upside-down T. The specimens with foam core (and a panel with this configuration as a reinforcement) requires only one lay-up and one cure cycle, being this the main advantage of this configuration.

One of the final steps of the specimens production was the ultrasonic inspection with a C-Scan. This technique uses a mechanical wave that is introduced into the part and is monitored as it travels

its assigned route through the part for any significant change [10]. Ultrasonic inspection is a very useful tool for the detection of internal delaminations, voids, or inconsistencies in composite components. However, these waves do not propagate in air or mediums of low density, which makes difficult to evaluate the results of the inspection of Sandwich components.

A Through-Transmission system with two transducers was used to analyze the specimens. The ultrasonic wave is transmitted from one transducer to the other by two water jets and the signal is then plotted to evaluate possible defects. The results from this study are presented in the next two figures.

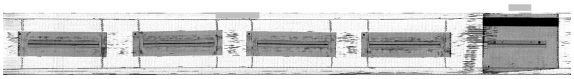

Figure 19: Ultrasonic inspection (T-Stiffener).

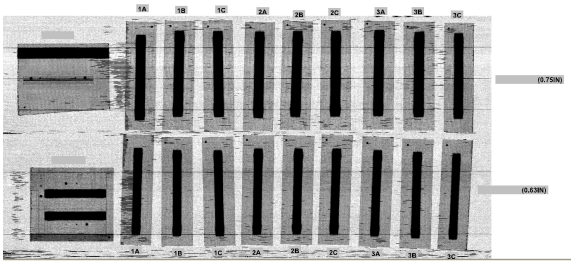

Figure 20: Ultrasonic inspection (stiffeners with BEAD).

In order to evaluate the specimens, two panels with standard defects were used. This panels show the maximum allowable defect that a structure may have without being rejected. However, it was not found any anomaly in the specimens.

The dark areas in Figures 19 and 20 represent the foam cores, through which the ultrasonic does not propagate. This is the reason why it is so difficult to find defects near these areas.

5. Conclusions

Changing the configuration of the stiffeners of the trailing edge panel of the wing would represent significant improvement of the manufacture process, with great advantages to OGMA. It not only reduces the number of fabrication steps but prevents future defects that may require reparations or even reject the entire panel.

Several methods were used to analyze the stiffeners. First, Classical Laminated Plate Theory, Finite Element Method and empirical formulas were employed to determined the axial and bending stiffnesses of each section. Then, it was determined the maximum load that each stiffener can support before fail, which was done with the Finite Element Method and the Maximum Strain Failure Criteria. Despite their simplicity and the approximations performed, these analyses allowed to prove that the two Sandwich configurations with foam core satisfy the requirements.

There was particularly interest in proving that the stiffener with the smallest core was able to provide enough mechanical resistance. As it was shown, the bending stiffness of the cross-section and the maximum load are higher than the ones of the current T-Stiffener. The analyses of the Sandwich configuration was made neglecting the foam core. This approximation made the computational analyses simpler.

Finally, a dimensional control of the Sandwich sections was performed in order to optimize the dimensions of the core.

Although the specimens were already manufactured, by the end of this work, the experimental tests haven't been performed.

References

[1] Armstrong, K.B., Bevan, L.G. and Cole, W.F. (2005), *Care and Repair of Advanced Composites*. SAE International, 2^{nd} edition.

[2] Kundu, A. K. (2010), *Aircraft Design*. Cambridge University Press, 489-493.

[3] Herakovich, C.T. (1998), *Mechanics of Fibrous Composites*. John Wiley & Sons, 307-324.

[4] Kassapoglou, C. (2010), *Design and Analysis of Composite Structures With Applications to Aerospace Structures*. John Wiley & Sons.

[5] Kaw, A.K. (2006), *Mechanics of Composite Materials*. Taylor and Francis Group, 2^{nd} edition.

[6] MIL-HDBK-17-3F (2002), *Composite Materials Handbook: Polymer Matrix Composites Materials Usage, Design, and Analysis - Volume 3*, U.S. Department of Defense.

[7] Reddy, J.N. (2003), *Mechanics of Laminated Composite Plates and Shells: Theory and Analysis*. CRC Press, 2^{nd} edition, 112-129.

[8] MIL-HDBK-17-2F (2002), *Composite Materials Handbook: Polymer Matrix Composites Materials Properties - Volume 2*, U.S. Department of Defense.

[9] *Theory Reference for The Mechanical APDL and Mechanical Applications*. ANSYS Inc., 7-29.

[10] *Aviation Maintenance Technician Handbook Airframe, Volume 1*. FEDERAL AVIATION ADMINISTRATION, U.S. Department of Transportation, 349-406.